Research Article

SOHAG JOURNAL OF SCIENCES

https://doi.org/10.21608/sjsci.2023.193578.1057

Amorphous Molybdenum Disulfide Thin Film for Photocatalysis and Gas Sensing Applications

Heba A. Mohamed*, H. M. Ali, H. A. Mohamed, and E. Kh. Shokr

Department of Physics, Faculty of Science, Sohag University, Sohag 82524, Egypt.
**E-mail: hebaabdelmoniem448@gmail.com*

Received: 13th February 2023**, Revised:** 8th March 2023**, Accepted:** 11th March 2023**.**
Published online: 6th April 2023

Abstract: Amorphous MoS_2 thin films have been prepared by thermal deposition on glass, quartz, and FTO substrates and investigated by UV-VIS – NIR spectroscopy. The type of substrate has a minor impact on the film's spectral absorption and band gap values. The investigation of MB – dye degradation by MoS_2 catalyst under UV – irradiation demonstrates high efficiency of 86%. MoS_2 films deposited on glass substrates have been experienced as CO_2, HCl, and I_2 gas sensors. The films revealed promises for CO_2 sensing at high temperatures (T≥300℃) in terms of relatively good response (~ 3 min) and moderate recovery of ~12 min. Besides, MoS_2 films revealed a quick response within 1 min for both HCl and I_2 gases, while their entire recovery needs a time period longer than one hour.
Keywords: Thermal evaporation technique, organic pollutants photodegradation, substrate type effect, gas sensing applications.

1. Introduction

The behavior of nanostructures differs greatly from that of the bulk structure of the same material [1–3]. According to the synthesis process, we can change nanostructure morphology, form, and phases to modify their functionalities. [3]. The advanced category of compounds named transition metal dichalcogenides (TMDCs) has a significant interest in the nanoworld [4-8] due to their excellent properties. Among the numerous TMDCs researched, MoS_2 has attracted huge attention recently due to its outstanding materials energy harvesting, nanoelectronic, and optoelectronic properties [9,10]. The Bulk of MoS_2 has a layered semiconducting structure primarily stacked hexagonally [11-13]. Each layer of MoS_2 consists of Molybdenum (Mo) atom bonded with two sulfur atoms (S) by a covalent bond, and week Vander Waal's force bonds layers, so it is easy to be mechanically separated and forming 2D MoS_2 nanostructures [12,14]. MoS_2 bulk has ~1.2 eV indirect bandgap, but it shifts upwards in energy to ~1.8 eV for monolayer structure due to a direct transition and varies depending on the nanostructure size [15-17].

The semiconductor photocatalytic process is a "Green technology" that enables the use of UV–VIS light to degrade organic contaminants [18-20]. The degradation of many types of dyes in water by UV- light irradiated semiconductors isutilized as an effective technique for purifying and recycling aqueouseffluents [21,22]. MoS_2 Semiconductor material has great attention in the photocatalytic field due to the tunable band gap, environmentally safe [14], low cost, good light absorption potentiality [23], fast carriers mobility [24], and vast surface area [25].

One of the most crucial electrical devices for detecting hazardous organic gases like methane, triethylamine, and benzene, as well as inorganic gases like CO_2, NO, NO_2, H_2, and NH_3, is a gas sensor [26-31]. Among the most desirable layered materials for the manufacture of a gas sensor is MoS_2, which has remarkable thickness-dependence electrical/chemical properties as well as an inherent high adsorption coefficient, high surface-to-volume ratio, and other favorable semiconducting characteristics [32-37].

In the present work, the thermal evaporation technique was used to deposit MoS_2 thin films with 300 nm thick on various types of substrates, including quartz, fluorine-doped tin oxide (FTO), and glass. Photocatalytic performance (PCP) of MoS_2 thin films as a catalyst for purifying water from the methylene blue (MB) as a model of contaminants has been investigated under UV irradiation. Substrate type effect on the MB- dye degradation under UV-irradiation has been studied. Additionally, MoS_2 thin films deposited on a glass substrate have been examined as gas sensors electrically for CO_2 detection and optically for HCl and I_2 detection.

2. Materials and methods

2.1. Preparation of MoS_2 thin films

Thermal evaporation is commonly used to deposit a uniform thin film with controlled thickness. 2N Molybdenum disulfide (MoS_2) in powder form was purchased from Sigma-Aldrich, that used to prepare the thin films. First, the powder was cold pressed in the form of tabletsless than 5 tons for 4 min. The substrates were cleaned by using an ultrasonic cleaner instrument (model EQ-VGT-1620QTD), using both acetone and distilled water. Then, a part of the tablet was brought in a coating unit (Edward's model; AUTO 306), and the chamber was evacuated to $\approx 4.2\times10^{-4}$ mbar. The film thickness and deposition rate were controlled by INFICON SQM – 160 thickness monitors (6 MH- with gold electrodes). The compressed tablets of MoS_2 were deposited on ultrasonically cleaned quartz, fluorine-doped tin oxide (FTO),

and glass substrates at a thickness of 300 nm. The deposition rate of (1 to 3 A0/sec) was maintained.

Using an x-ray diffractometer (Philips model PW1710 with Cu as the target and Ni as a filter, λ =1.5418 nm, Holland), MoS_2 thin films of 300 nm thick deposited on glass, FTO and quartz substrates were investigated by adjusting the diffraction angle (2θ) from 10 to 80 by a 0.04 step width. The x-ray diffractometer operates at a 40KV accelerating voltage, 30 mA current, and a 20/min scanning speed.

2.2. Photocatalytic performance (PCP) of MoS_2 thin films

A Jasco V-570 UV-visible-NIR spectrophotometer was utilized to measure the absorbance, transmittance, and reflectance spectra in the wavelength range of 200-2500 nm at normal incidence. This instrument has photometric accuracy of 0.3% transmittance or 0.002-0.004 absorbance. Photocatalytic performance (PCP) of MoS_2 thin films was examined towards Methylene Blue (MB) dye as an example of water contaminants. MoS_2 thin films were immersed in 30 ml MB dye solution of 10 ppm concentration. This solution was kept in the dark for 1 hour, and the initial MB dye absorbance value (A_o) was determined. Then, the solutions were exposed to UV-light (UV-C Germicidal lamps having a major emission wavelength of 254 nm) for a total time period of 280 min by successive intervals of 5 min. The MB dye absorbance value (A_t) was recorded after each time interval of 5 min.

2.3. Gas sensing performance (GSP) of MoS_2 thin films

A two-probe technique is used to measure the film resistance using a multimeter (model hp HEWLETT-PACKARD34401). The electrodes were made on the film surface using silver paste with an apart distance of about 3 mm. The films were then placed in a software furnace tube's center to adjust the sample temperature over the range of 0-4000 C by step of 100 C.

MoS_2 thin films deposited on a glass substrate were electrically investigated as a CO_2 gas sensor at different temperatures (250, 290& 300^0C). The gas flow rate was controlled using flow meter apparatus (Aera ROD-4) at 8.4 SCC/minute (which is equivalent to 140 bubbles/ minute). Then, at first, the samples' resistance was recorded in the air (reference gas) at a temperature of 250^0 C until the resistance becamestable. These samples were exposed to CO_2 gas (target gas) for 18 min. Finally, these films were again exposed to surrounding air, and their resistance was recorded. The system temperature was maintained constant at 250° C throughout the testing process to avoid thermal resistance variations. The same procedure was followed at higher temperatures of 290and 350^0 C too.

Moreover, MoS_2 thin films were optically investigated as gas sensors for HCl and I_2 gases. In order to identify the response and recovery times, the absorbance spectrum of the film was recorded before and after gas exposure at different successive interval periods.

3. Results and Discussion

3.1. Structural analysis for MoS_2 thin films

Fig. 1 shows XRD, SEM, and EDX analyses of the present MoS_2 – material. All of the peaks revealed in X-ray diffractograms (Fig. 1a) correspond to MoS_2 powdered material. The relatively more intense peaks of (002), (100), (013), and (015) are observed at the scattering angles of 14.397°, 32.686°, 39.557°, and 49.807°, respectively. The obvious preferred crystallization orientation through the (002) plane could correspond to MoS_2 hexagonal structure, with lattice constants of a = b = 3.161Å and c = 12.295 Å.

SEM image (Fig. 1b) illustrates an almost uniform distribution of different separatedgrains in shapes grains, volumes, and orientations on the sample surface, which could be correlated to the different observed XDR – peaks (Fig. 1a). Fig (1c) illustrates the corresponding EDX of each of MoS_2 powdered samples. The presences of Mo, O & S are identified, respectively.

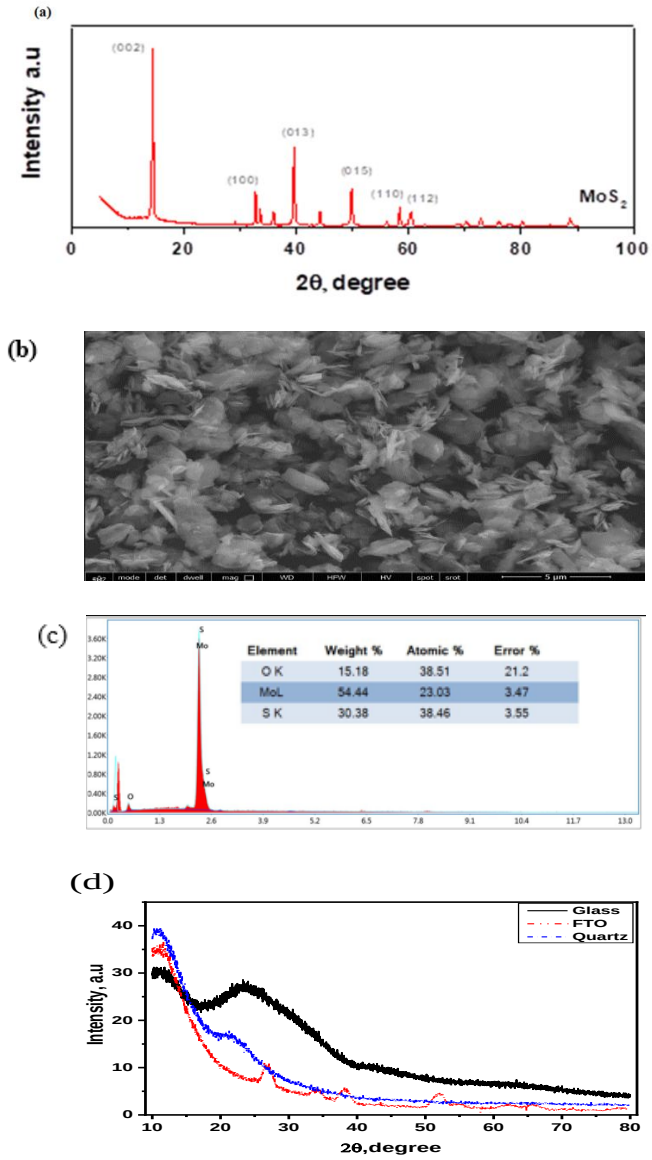

Fig. 1: XRD (a) SEM (b) EDX (c) of powdered MoS_2 and (d) XRD of MoS_2 thin film on different substrates.

Fig. 1d displays the X-ray diffraction patterns of MoS_2 thin films deposited on various substrate types, including glass, FTO, and quartz. As shown, there are no diffraction peaks characterizing the present MoS_2 material that can be observed. All the observed diffraction peaks correspond to the FTO-coated glass substrate due to its polycrystalline nature. This indicates that all films have an amorphous structure, which may be attributed to the films' rapid quenching to room temperature after the deposition process.

3.2. Optical characterization of MoS_2 samples

Fig.2 depicts the optical absorption spectra of MoS_2 films deposited on different substrates. As shown, the change in film substrates causes a small difference in the spectral behavior of the film absorption in terms of a small difference in absorption intensities over the whole spectral range and a slight shift of the absorption edge. Accordingly, the optical band gap (E_g) values calculated roughly using the sloping part of the end absorption of the fundamental absorption edge [38] are also slightly affected by the substrate type. On the basis of the Tauc equation [39], these roughly estimated E_g – values were employed to determine both the electron transition type and the more precise values of E_g as described elsewhere [40]. The accurate values of E_g with direct allowed transition were and recorded in Table 1.

3.3. Photocatalytic performance (PCP) under UV-irradiation

Fig.3 shows the absorption spectra characterizing MB dye degradation under the UV- irradiation and MoS_2-catalyst. The dye degradation was observed as a gradual decrease in the intensity of the absorption peak at 657 nm with time. It was observed that the degradation of MB dye increases with the increase of illumination time. Besides, the best degradation under UV- light entirely in 280 min was recorded for quartz substrate compared to glass and FTO substrates.

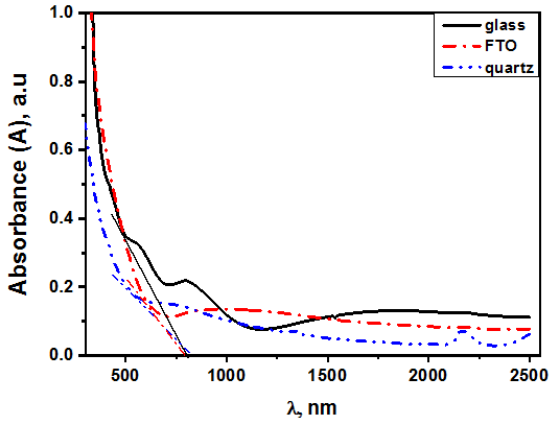

Fig. 2: Absorbance spectrum of 300 nm thick MoS_2 thin film deposited on glass, FTO, and quartz substrates.

The dye degradation was controlled in terms of degradation efficiency ($\eta\%$) given by the following equation:

$$\eta = \frac{A_o - A_t}{A_o} \times 100 \qquad (1)$$

where $A_o \& A_t$ are the initial and the specified time irradiation absorbance values, respectively.Fig. 4ashows the effect of UV-irradiation time (t) on MB dye degradation efficiency. The best value $\eta = 86\%$ of degradation efficiencywas observed for the film deposited on quartz substratewhile for glass, and FTO substrates η was 82%, and 73%, respectively.

The degradation reaction kinetics of the MB dye performed by MoS_2 thin films was estimated by the pseudo- first-order kinetic model given by the Eq. (2) [41]:

$$\ln\left(\frac{A_t}{A_o}\right) = -kt \qquad (2)$$

where k (min^{-1}) represents the first-order of a rate constant and t is UV- irradiation time.Fig. 4bshows the photodegradation process of MBdye and the photodegradation rate for MoS_2 thin films (Fig. 4inset) deposited on glass, FTO and quartz substrates under UV- irradiation. It was observed that the film deposited on a quartz substrate revealed the highest photodegradation rate constant $(k = 0.00644 min^{-1})$ while the values$(k = 0.00586\ min^{-1})$, and $(k = 0.00451 min^{-1})$ were obtained for the films deposited on glass, and FTOsubstrates, respectivily.

The half-life time $t_{1/2}$ (min), needed to reduce the concentration of MB dye in solution to its half initial value, is calculated as follows:

$$t_{1/2} = \frac{ln\,2}{k} \qquad (3)$$

The performance of the photodegradation process could be certified through a figure of merit $\varphi_{perf}(min^{-1})$ that is directly and inversely related to the photocatalytic efficiency and half life time, respectively and estimated by,

$$\varphi_{perf} = \eta \,/\, t_{\frac{1}{2}} \qquad (4)$$

The obtained results of the photodegradation process under UV- irradiation are summarized and compared with the corresponding reported results as shown in Table (1). As demonstrated, the degradation efficiency values of MoS_2 films deposited on glass and quartz substrates are as high as 82- 86% attained at relatively long times (Table 1), leading to relatively low performance. This may be attributed to the quick recombination of the generated electron - hole pairs at the active sites of the unsaturated Mo and S atoms at the S – Mo – S edges [42,43]. The small difference in the effect of substrates on the photodegradation performance (under UV- irradiation) may be due to the slight change in the band gap value induced by the substrates and consequently leads to small difference in light harvesting. This leads to an inefficient difference in $e^- - h^+$pairs generation demanded for the dye- degradation reaction process.

The photodegradation reaction mechanism can be achieved as follows [44]:

The free electron received by O_2 dissolved in water can form free radicals $\cdot O_2^-$.

$$\text{i.e} \quad e^- + O_2 \rightarrow \cdot O_2^- \qquad (5)$$

Due to its negative side $(\bar{\delta}, O)$ the polar molecules of water can be attracted by the free holes producing $\cdot OH$ radicals with protons, H^+.

$$\text{i.e.} H_2O + h^+ \rightarrow \cdot OH + H^+ \quad (6)$$

Both H^+ species and dissolved $\cdot OH$ can diffuse towards the opposite side and recombine with electrons resulting in hydrogen peroxide (H_2O_2).

Then, the H_2O_2 – polar molecules and $\cdot OH$ radicals can receive an electron, where

$$H_2O_2 + H^+ + e^- \rightarrow \cdot OH + H_2O \quad (7)$$

Finally;

$$MB\ (dye) + \cdot O_2^- / \cdot OH \rightarrow CO_2 \uparrow + H_2O + non - \text{toxic products degradation} \quad (8)$$

3.4. Gas sensing performance (GSP) of MoS_2 thin films

The DC-electrical resistance (R) for MoS_2 thin films with 300 nm thick deposited on glass substrates within temperature range 463–673 K was depicted in Fig. 5a. As illustrated, the DC-resistance gradually declines as the temperature increases indicating semiconducting conduction behavior [47]. Such conduction behavior can be described through the thermal variation of the film conductivity (σ_{DC}) according to the following Arrhenius relation:

$$\sigma_{DC} = \sigma_o exp\left(\frac{-E_\sigma}{k_B T}\right) \quad (9)$$

, where σ_o is the pre-exponential factor, K_B is the Boltzmannconstant, and E_σ is the conduction activation energy. The linear relationship of $ln\ \sigma_{DC}$ vs. $1/T$ plot (Fig. 5, b) suggests that the conductivity in the considered range of temperatures has been thermally activated [48]. Comparing the obtained values of the activationenergy ($\Delta E_\sigma = 0.078\ eV$) and the energy band gap ($E_g = 1.53\ eV$) confirms the intrinsic conduction predominance, where $E_g \cong 2\Delta E_\sigma$.

To examine and contrast the CO_2 sensing characteristics of the pristine MoS_2 samples, they were exposed to 7.2 SCC/min of CO_2 at different temperatures (250, 290, and 300^{0}C). Asshown in Fig. 6 at relatively lower (250& 290^{0}C) values of temperature the films did not respond to CO_2 gas. However, the resistance of the MoS_2 increases immediately when CO_2 introduced into the testing furnace tube at 300^o C and as the gas stopped it more slowly increases within ~23 min due to the adsorption of the residual gas in the tube, then gradually decreases reaching its low equilibrium value during ~ 12 min.This indicates that MoS_2 films can respond to CO_2 at values of temperature as high as 300^o C with reversibility during~12 min. Such moderate sensing sensitivity may be due to the small difference between the film resistivity (ρ_{gas}) and (ρ_{air}) after and before gas exposure, respectively. The difference (ρ_{gas}- ρ_{air}) must be high enough to achieve high sensor sensitivity. The elevating of measuring temperature (T ≥ 300^{0}C) results in the film resistance decrease leading to the increment of the ρ_{gas}- ρ_{air} difference, a matter that can improve the sensor response and coverage processes.

This suggests that such films are promising candidates for high temperature CO_2 – sensing.

The investigation of MoS_2 thin films deposited on glass substrates as HCl and I_2 optical sensors was experienced. The variation of the optical absorbance spectra of MoS_2 thin films on glass substrates as a result of exposure to HCl, and I_2 gases

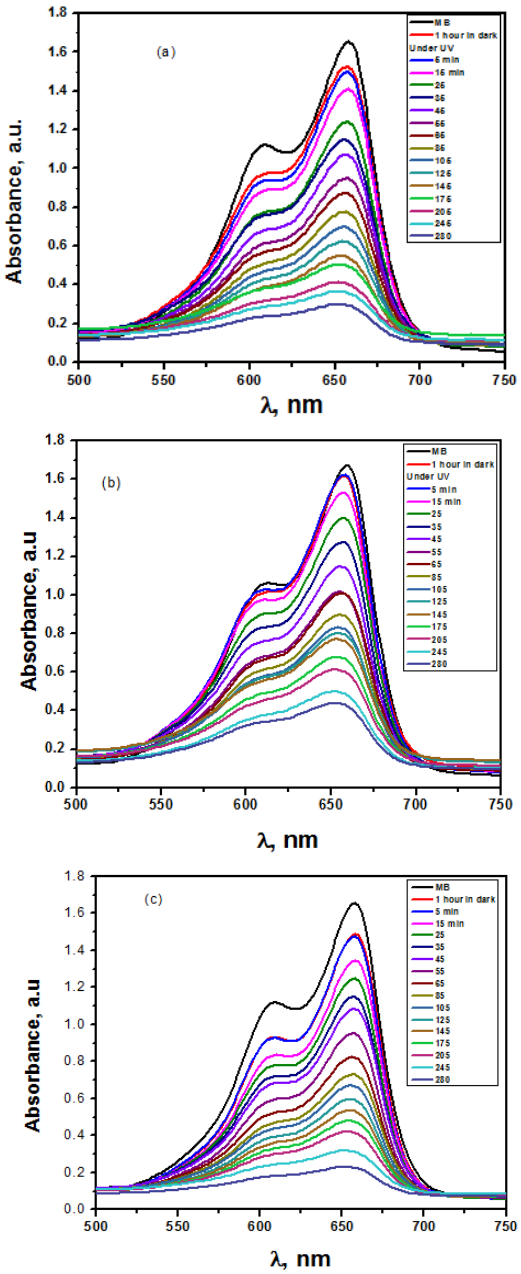

Fig. 3: MB dye photodegradation under UV – light irradiation MoS_2 thin films of 300 nm thick deposited on glass (a), FTO (b) and quartz (c), substrates at different irradiation time.

are depicted in Figs. 7,8, respectively. It was observed that the absorbance spectra improved and the absorption edge shifted towards longer λ – valueswith prolongation the exposure time to 1 hour, showing a good response within 1 min and relatively long recovery time for both HCl and I_2 gases.

To confirm the results of HCl and I_2 sensing, the Urbach energy (E_u) can be employed in the range of $\alpha < 10^4$ Cm^{-1}, where:

$$\alpha = \alpha_o + e^{\frac{h\nu}{E_u}} \quad (10)$$

or

$$ln\ (\alpha) = \frac{h\nu}{E_u} + ln\ (\alpha_o) \quad (11)$$

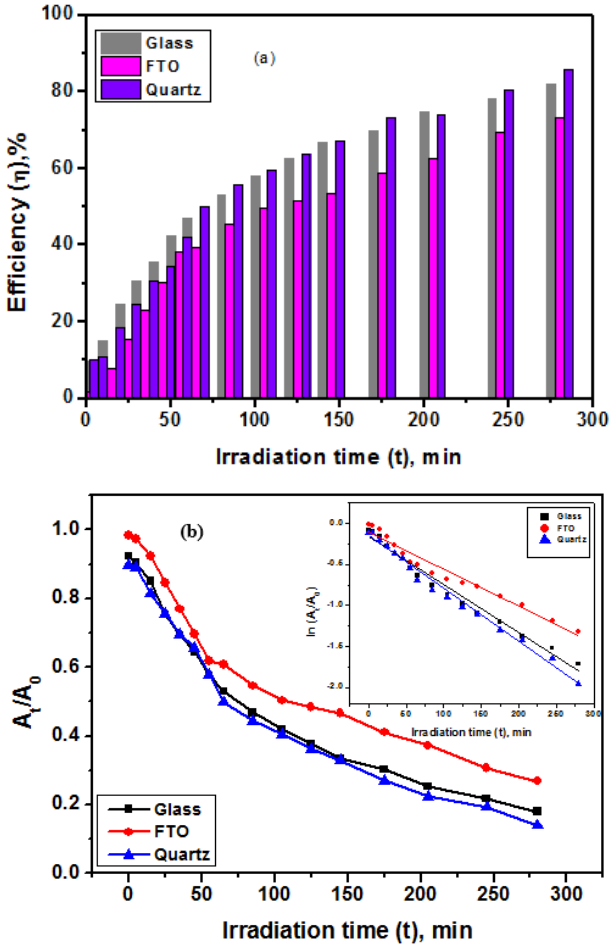

Fig. 4: Photocatalytic efficiency (a) and photodegradation activity (A_o/A_t)& rate ($ln\ A/A_o$) - inset (b) as functions of UV - irradiation time.

Table 1: Comparison results of the present work results with others reported for various photodegradation strategies.

Illumination light	UV				VIS	
catalyst	MoS_2			MoS_2 QDs/ZnO	V_2O_5	V_2O_5
Substrate type	Glass	FTO	Quartz			
dye	MB			RhB	MB	MO
Degradation time	280 min			30 min dark+50 min irradiation	300 min	300 min
E_g, eV	1.53	1.55	1.51			
k, min^{-1}	0.0059	0.0045	0.0064	0.0571	0.0811	0.1193
$t_{\frac{1}{2}}$, min	118.28	153.69	107.63	12.14	8.546	5.80
η %	82	73	86	95	24	48
φ_{perf}, min^{-1}	0.69	0.47	0.79	7.829	2.80	8.26
Ref	Present work			[45]	[46]	

where α_0 is a constant and E_u is a measure of the energy width of the localized states band tails in the band gap.

The calculated values of E_u from the slopes of $ln(\alpha)$ *vs.* hv plots (Fig. 9) are given in Table 2. As shown, the value of E_u increases with HCl gas absorption and decreases with gas release. The opposite behavior is observed in the case of I_2. This could be because HCl and I_2 are reducing and oxidizing gases, respectively. Furthermore, despite the apparent rapid response of films (within 1 minute) to both HCl and I_2 gases, their recovery is extremely slow. The entire recovery for each case requires a time period longer than 1 hour.

Table 2: Urbach energy (E_u) variations with gas exposure and releasing times.

Film case	E_u	
	HCL	I_2
As	0.781	1.300
60 min in I_2 or HCL	1.095	0.979
60 min of gas releasing in air	1.027	1.120

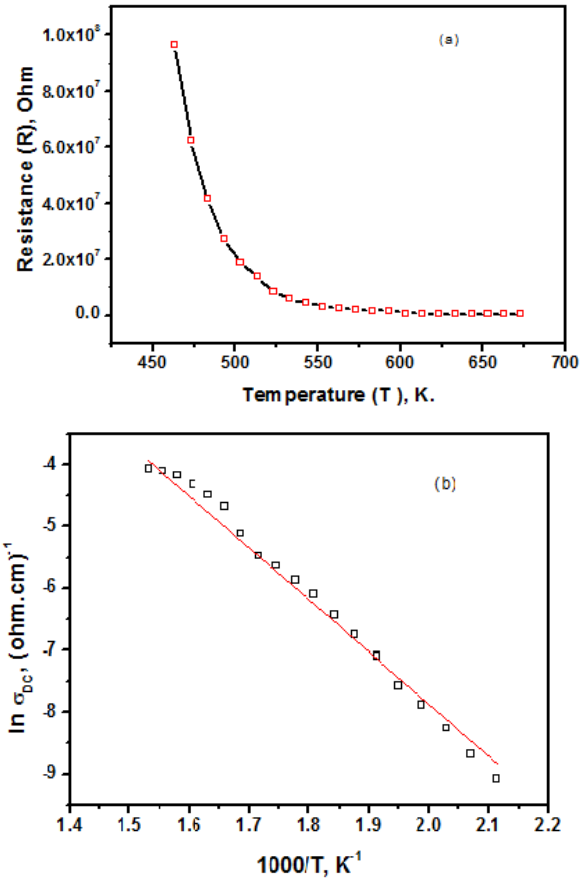

Fig.5: The DC-electrical resistance (a) and $ln(\sigma_{DC})$ *vs.* $(1000/T)$, of MoS_2 thin films with 300 nm thick deposited on glass substrates.

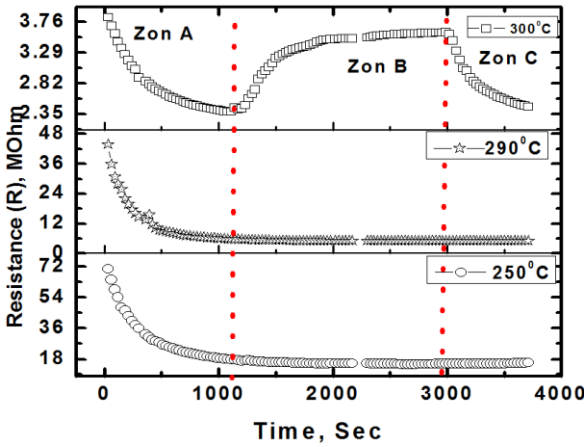

Fig. 6: The sensing performance of MoS_2 thin films with 300 nm thick deposited on glass substrates towards CO_2 at different temperatures.

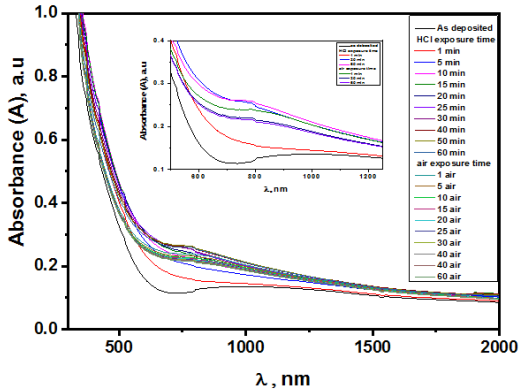

Fig. 7. The variation of the optical absorptance spectra of MoS_2thin films with 300 nm thick deposited on glass substrates with HCl gas exposure time.

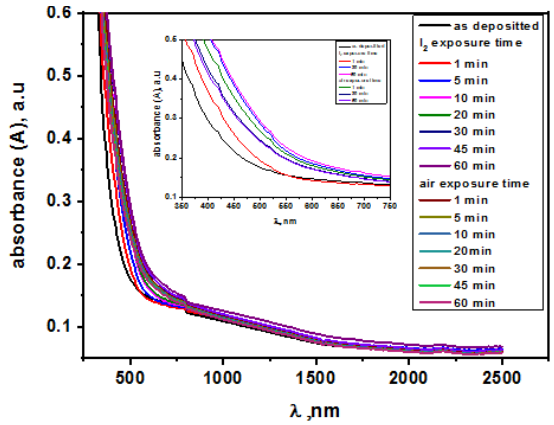

Fig. 8. The variation of the optical absorptance spectra of MoS_2thin films with 300 nm thick deposited on glass substrates with I_2 gas exposure time.

Summary and conclusions

Thin MoS_2 films have been synthesized on glass, FTO and quartz substrates using the thermal evaporation technique. The microstructure, morphology and chemical constituents were analyzed and identified for powder MoS_2 samples via XRD, SEM and EDX. The amorphous structure of all the considered films has been proven by X-ray diffraction analysis. The optical UV – VIS – NIR spectral measurements indicated the minor effect of substrate type on the film spectral absorption intensity and band gap values.

The efficiency of organic photodegradation achieved in 280 min by MoS_2 films deposited on quartz substrates under UV - irradiation is as high as 86%, suggesting the possibility of its utility for purification of water from organic pollutants.

MoS_2 films deposited on glass substrates proved their validity to be applied as CO_2 gas sensors at high temperatures (T), which offers a high enough difference in the film resistivity before and after gas exposure and consequently improves its sensitivity. For both gaseous HCl and I_2 which act as reducing and oxidising gases, respectively, the MoS_2 films manifested a relatively good response of 1 min with a recovery period longer than 1 hour.

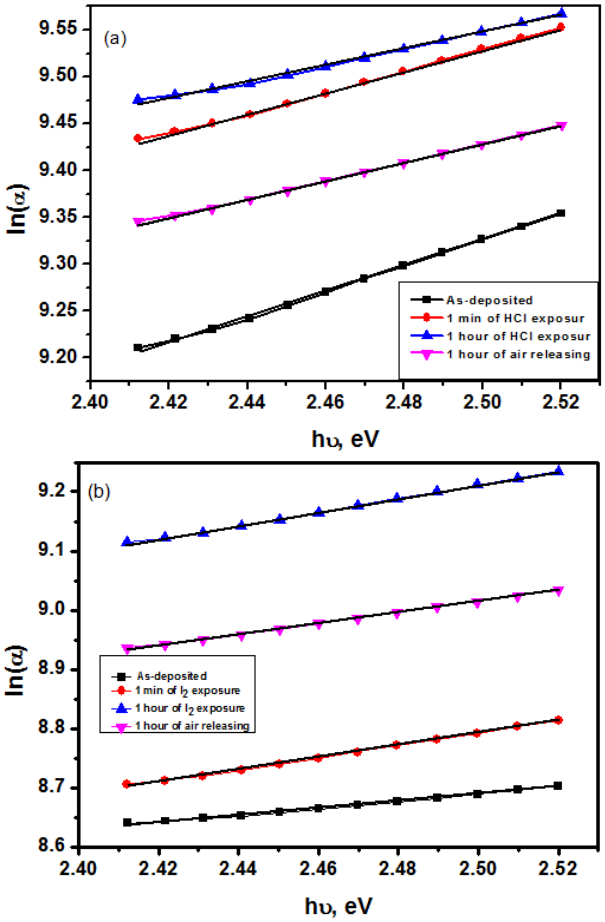

Fig. 9: $ln(\alpha)$vs. $h\upsilon$plots of MoS_2thin films at differentHCl (a), and I_2 (b) gas adsorption and releasing time periods.

References

[1] Q. Zhang, E. Uchaker, S.L. Candelaria, G. Cao,*Chemical Society Reviews* 42 (2013) 3127-3171.

[2] K. Maeda, K. Domen,*The Journal of Physical Chemistry Letters* 1 (2010) 2655-2661.

[3] X. Wang, S. Jin, H. An, X. Wang, Z. Feng, C. Li,The *Journal of Physical Chemistry C* 119 (2015) 22460-22464.
[4] K. Nayana, A. Sunitha, *Materials Today: Proceedings* 45 (2021) 4671-4676.
[5] J. Lu, H. Liu, E.S. Tok, C.-H. Sow, *Chemical Society Reviews* 45 (2016) 2494-2515.
[6] G. Eda, H. Yamaguchi, D. Voiry, T. Fujita, M. Chen, M. Chhowalla, *Nano letters* 11 (2011) 5111-5116.
[7] M. Chhowalla, H. Shin, G. Eda, L. Li, K. Loh, H. Zhang, The chemistry of 2D layered transition metal dichalcogenide nanosheets Nat, in, Chem, 2013.
[8] X. Li, H. Zhu, J. Materiomics 1 (2015) 33–44.
[9] Y. Huang, J. Guo, Y. Kang, Y. Ai, C.M. Li, *Nanoscale* 7 (2015) 19358-19376.
[10] S. Mukherjee, Z. Ren, G. Singh, *Nano-micro letters*, 10 (2018) 1-27.
[11] N.H. Attanayake, A.C. Thenuwara, A. Patra, Y.V. Aulin, T.M. Tran, H. Chakraborty, E. Borguet, M.L. Klein, J.P. Perdew, D.R. Strongin, *ACS Energy Letters* 3 (2017) 7-13.
[12] A. Sunitha, P. Praveen, M. Jayaraj, K. Saji, *Optical Materials* 85 (2018) 61-70.
[13] J. Ali, G.U. Siddiqui, K.H. Choi, Y. Jang, K. Lee, J*ournal of Luminescence* 169 (2016) 342-347.
[14] N. Alinejadian, L. Kollo, I. Odnevall, M*aterials Science in Semiconductor Processing* 139 (2022) 106331.
[15] Y. Qi, Q. Xu, Y. Wang, B. Yan, Y. Ren, Z. Chen, ACS nano, 10 (2016) 2903-2909.
[16] Q. Xiong, T. Shimada, T. Kitamura, Z. Li,Science China *Physics, Mechanics & Astronomy* 63 (2020) 114611.
[17] M. Mortazavi, C. Wang, J. Deng, V.B. Shenoy, N.V. Medhekar, *Journal of Power Sources* 268 (2014) 279-286.
[18] M.R. Hoffmann, S.T. Martin, W. Choi, D.W. Bahnemann, *Chemical reviews* 95 (1995) 69-96.
[19] X. Chen, S. Shen, L. Guo, S.S. Mao, *Chemical reviews* 110 (2010) 6503-6570.
[20] H. Tong, S. Ouyang, Y. Bi, N. Umezawa, M. Oshikiri, J. Ye, *Advanced materials* 24 (2012) 229-251.
[21] H. Lachheb, E. Puzenat, A. Houas, M. Ksibi, E. Elaloui, C. Guillard, J.-M. Herrmann, *Applied Catalysis B: Environmental* 39 (2002) 75-90.
[22] C. Han, M. Pelaez, V. Likodimos, A.G. Kontos, P. Falaras, K. O'Shea, D.D. Dionysiou, *Applied Catalysis B: Environmental*, 107 (2011) 77-87.
[23] W.R. Divigalpitiya, S.R. Morrison, R. Frindt, *Thin Solid Films* 186 (1990) 177-192.
[24] D.B. Sulas-Kern, E.M. Miller, J.L. Blackburn, *Energy & Environmental Science* 13 (2020) 2684-2740.
[25] C.-H. Jiang, C.-B. Yao, L.-Y. Wang, X. Wang, Z.-M. Wang, H.-T. Yin, *Journal of Luminescence* 255 (2023) 119546.
[26] B. Timmer, W. Olthuis, A. Van Den Berg, *Sensors and Actuators B: Chemical* 107 (2005) 666-677.
[27] X. Liu, T. Ma, N. Pinna, J. Zhang, *Advanced Functional Materials* 27 (2017) 1702168.
[28] M.V. Nikolic, V. Milovanovic, Z.Z. Vasiljevic, Z. Stamenkovic, *Sensors* 20 (2020) 6694.
[29] X. Liu, S. Cheng, H. Liu, S. Hu, D. Zhang, H. Ning, *Sensors* 12 (2012) 9635-9665.
[30] Z. Li, C. Brouwer, C. He,Chemical reviews, 108 (2008) 3239-3265.
[31] T. Hübert, L. Boon-Brett, G. Black, U. Banach, *Sensorsand Actuators B: Chemical* 157 (2011) 329-352.
[32] F.K. Perkins, A.L. Friedman, E. Cobas, P. Campbell, G. Jernigan, B.T. Jonker, *Nano letters* 13 (2013) 668-673.
[33] M. Donarelli, L. Ottaviano, *Sensors* 18 (2018) 3638.
[34] W. Zhang, P. Zhang, Z. Su, G. Wei, *Nanoscale* 7 (2015) 18364-18378.
[35] C. Rao, K. Gopalakrishnan, U. Maitra, *ACS applied materials & interfaces* 7 (2015) 7809-7832.
[36] P.K. Kannan, D.J. Late, H. Morgan, C.S. Rout, *Nanoscale* 7 (2015) 13293-13312.
[37] R. Kumar, N. Goel, M. Kumar, NO_2 sensing at room temperature using vertically aligned MoS*2* flakes network, in: AIP Conference Proceedings, AIP Publishing LLC, (2018) 060006.
[38] K.F. Mak, C. Lee, J. Hone, J. Shan, T.F. Heinz, *Physical review letters*, 105 (2010) 136805.
[39] P.K. Nayak, N. Periasamy, *Org. Electron*. 10 (2009) 1396–1400.
[40] E. K. Shokr, M.S. Kamel, M. S., H. Abdel-Ghany & M. A. E. A. A. Ali, *Optik* 243 (2021), 167385.
[41]Y., Zheng, J., Wang, Y.,Wang, Y., H., Zhou, Q., Yang, & W., Huang, *Molecules* 25 (2019), 2.
[42] Y.J. Yuan, H.W. Lu, Z.T. Yu, Z.G. Zou, *ChemSusChem*, 8 (2015) 4113-4127.
[43] Y. Liu, J. Kong, J. Yuan, W. Zhao, X. Zhu, C. Sun, J. Xie,*Chemical Engineering Journal* 331 (2018) 242-254.
[44] A. F., Cabrera, C. R., Torres, S. G., Marchetti, & S. J. Stewart, *Journal of Environmental Chemical Engineering* 8(2020) 104274.
[45] R. Gang, L. Xu, Y. Xia, J. Cai, L. Zhang, S. Wang, R. Li,*Journal of Colloid and Interface Science* 579 (2020) 853-861.
[46] S.K. Jayaraj, V. Sadishkumar, T. Arun, P. Thangadurai,*Materials Science in Semiconductor Processing*85 (2018) 122-133.
[47] S. Kumar, B. Lal, S. Rohilla, P. Aghamkar, M. Husain,*Journal of alloys and compounds*505 (2010) 135-139.
[48] H. Ali, S. Saleh,*Thin Solid Films* 556 (2014) 552-559.